In-plane shear response of steel-concrete composite shear walls: results of experiments

Nguyen NH[1], Epackachi S[1], Kurt EG[2], Whittaker AS[3], Varma AH[4]

1) PhD Candidate, Dept. of Civil, Structural and Environmental Engineering, University at Buffalo, NY, USA 14260
2) PhD Candidate, School of Civil Engineering, Purdue University, IN, USA 47907
3) Professor and Chair; Director, MCEER; Dept. of Civil, Structural and Environmental Engineering, University at Buffalo, NY, USA 14260
4) Associate Professor, School of Civil Engineering, Purdue University, IN, USA 47907

Email: Nam H. Nguyen (namnguye@buffalo.edu)

Abstract

Steel-concrete (SC) composite walls are being used for the construction of containment internal structures and shielding structures in nuclear power plants. SC walls are composed of steel faceplates, connectors and infill concrete, where the connectors are typically constructed from cross-wall tie rods and shear studs welded to the faceplates. The experimental and analytical in-plane shear behaviors of four large-size SC walls are summarized in this paper. A focus is the inelastic range of response, which is expected for beyond design basis shaking of nuclear power plant structures and design basis shaking of building structures. A number of design parameters are investigated, including infill concrete thickness, reinforcement ratio, stud spacing, and tie bar spacing. The SC wall specimens were subjected to cyclic in-plane loading. The experimental force-displacement responses and damage to the steel faceplates and infill concrete are documented. Nonlinear FE analysis was performed using ABAQUS. The numerical results are in good agreement with the physical experiments. Numerical experiments are expanding the design space to enable prescriptive recommendations to be made for codes and standards for safety-related nuclear structures and buildings.

Keywords: Steel-concrete composite shear walls, earthquakes, experiments, in-plane response

1. INTRODUCTION

Steel-concrete (SC) composite walls have been under extensive research since 1980s (Fukumoto et al., 1987). Subsequently, the researchers from Japan, Korea, United Kingdom, and the United States have contributed to the understanding of the behavior of SC walls (e.g., Kaneuji et al., 1989; Sasaki et al., 1995; Takeda et al., 1995; Ozaki et al., 2004; Varma et al., 2011). In Japan, technical guidance on the design of SC walls was issued in 2005 (JEAG-4618, 2005). In the United States, a draft specifications for SC walls is currently under review by American Institute of Steel Construction as an appendix to AISC N690 (2006).

SC walls are being used for the construction of containment internal structures and shielding structures in large light water reactors in the United States and abroad. SC walls have been proposed for other nuclear construction, including small modular reactors. Although the elastic response of SC walls under in-plane loading is reasonable well understood (and just as well

understood as reinforced concrete construction), information on post-elastic (inelastic) response is minimal because the focus of nuclear power plant design has been elastic response for design basis earthquake shaking.

The failures at the Fukushima Daiichi nuclear power plant in 2011 and recent initiatives from the US Nuclear Regulatory Commission in the aftermath of the Great East Japan Earthquake in 2011 have emphasized the importance of understanding component and system behavior for earthquake shaking more intense than design basis.

This paper addresses the response of SC walls under beyond design basis loadings. The scope of the experimental program is limited to four specimens. Only in-plane loading is considered. Many additional tests will have to be undertaken to fully understand the seismic response of SC walls through failure under in-plane and out-of-plane loadings and to validate numerical models and tools for the purpose of design and assessment. The following sections of the paper describe the testing program and present key experimental results, damage data, and conclusions. Preliminary results obtained from FE analysis of the walls are presented.

2. EXPERIMENTAL PROGRAM

Test specimen description

Four large-size specimens (SC1 through SC4) were built and tested under displacement-controlled cyclic loading. The tests were conducted in the NEES laboratory at the University at Buffalo with support from the Bowen Laboratory at Purdue University. The design variables considered in the testing program include reinforcement ratio, tie-rod and stud spacing. The aspect ratio (height-to-length, H / L) of all walls was 1.0. Information on the four walls is provided in Table 1. In this table, studs and tie rods serve on connectors, spaced at distance S, the overall thickness of the wall is T, the thickness of each faceplate is t_p, the reinforcement ratio is $2t_p / T$, the stud spacing ratio is S / t_p.

Table 1. Test specimen configurations

Specimen	Wall dimension ($H \times L \times T$) (in. × in. × in.)	Stud spacing (in.)	Tie rod spacing (in.)	Reinforcement ratio (%)	Faceplate slenderness ratio	Day-of-test wall concrete strength (ksi)
SC1	60×60×12	4	12	3.1	21	4.5
SC2	60×60×12	-	6	3.1	32	4.5
SC3	60×60×9	4.5	9	4.2	24	5.3
SC4	60×60×9	-	4.5	4.2	24	3.9

The diameter of the studs and tie rods was 0.375 in. for all walls; the studs and tie rods were fabricated from 50 ksi steel. The yield and ultimate strengths of the steel faceplates calculated from three coupon tests, were 38 and 55 ksi, respectively. The nominal compressive strengths of the infill concrete and the foundation concrete were 4 and 6 ksi, respectively.

Each SC wall was installed on top of a re-usable foundation block. The base of each wall included a 1-in. thick base plate to which the faceplates were CJP groove welded. Two rows of 13 number 0.675-in. diameter studs were welded to the base plate to bond the concrete and improve the transfer of shearing and tensile forces. The base plate was installed atop a 1-in. thick base plate embedded in the foundation block and was secured to the foundation block

using 22 1.25-in. diameter threaded B7 bars that were post-tensioned to 100 kips per bar. Figure 1 is a photograph of SC1 installed on the foundation block.

Figure 1. Specimen SC1

Instrumentation

Krypton light emitting diodes (LEDs), rosette strain gages, linear potentiometers, Temposonic displacement transducers, and linear variable displacement transducers were used to collect data. String potentiometers and Temposonics were attached to the ends of the wall to measure the in-plane displacement of the walls. Four string potentiometers measured out-of-plane displacement; one at each corner of the specimen. Linear potentiometers and the Krypton LEDs measured the horizontal and vertical displacements of the foundation block relative to the strong floor.

The Krypton system was used to monitor the 3D displacements of the wall specimens. LEDs were attached to one steel faceplate. Rosette strain gages were installed at three elevations on the other faceplate. The positions of the LEDs and strain gages on SC3 are presented in Figure 3. The applied load was calculated as the sum of the in-plane components of the actuator forces.

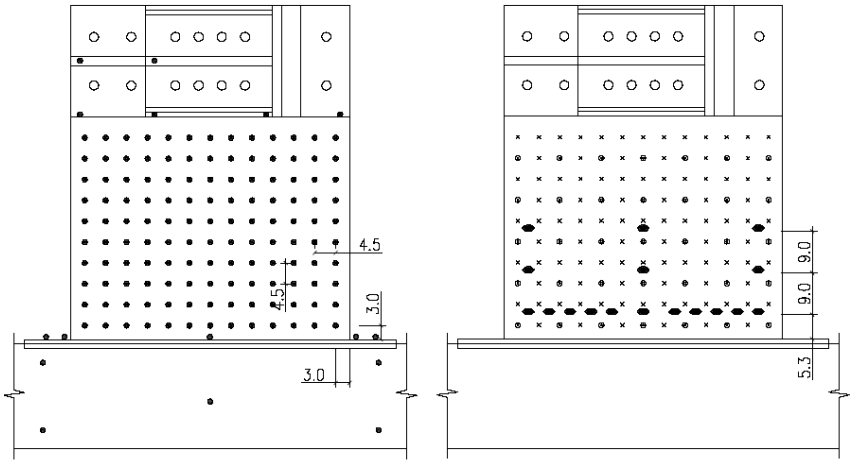

(a) Krypton LEDs (b) Rosette strain gages

Figure 3. Krypton LEDs and strain gages on SC3

Test setup

Two horizontally inclined high force-capacity actuators were used to apply cyclic lateral loads to the top of the SC walls. The foundation block was post-tensioned to the strong floor with 14

number 1.5 in. diameter Dywidag bars to prevent foundation movement during testing. The test setup is shown in Figure 2.

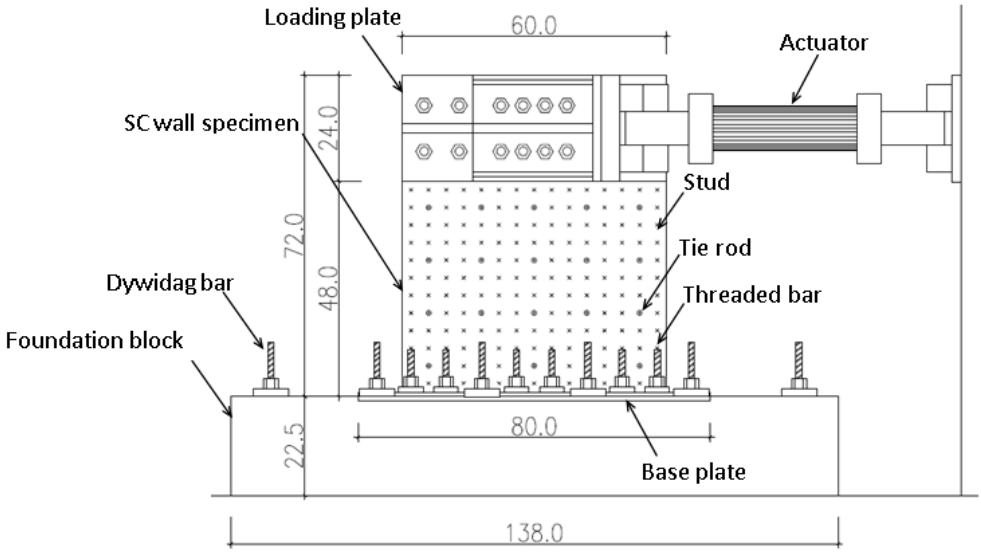

Figure 2. SC wall test setup

Load protocol

Displacement controlled cyclic loads were imposed on each wall. No axial load was applied. The loading protocol is presented in Table 2. Peak deformations at each load step were based on a reference displacement of 0.14 in, estimated from pretest analysis of the walls. Each load step had two cycles. The loading speed was 0.01 in./sec.

Table 2. Loading protocol for SC walls

Load step	Peak deformation (in)	Number of cycles	Description
LS1	±0.014	2	10% ref. disp.
LS2	±0.07	2	50% ref. disp.
LS3	±0.105	2	75% ref. disp.
LS4	±0.14	2	100% ref. disp.
LS5	±0.28	2	200% ref. disp.
LS6	±0.42	2	300% ref. disp.
LS7	±0.56	2	400% ref. disp.
LS8	±0.7	2	500% ref. disp.
LS9	±0.84	2	600% ref. disp.
LS10	±0.98	2	700% ref. disp.
LS11	±1.12	2	800% ref. disp.
LS12	±1.26	2	900% ref. disp.
LS13	±1.4	2	1000% ref. disp.
LS14	±1.68	2	1200% ref. disp.
LS15	±1.96	2	1400% ref. disp.

Experimental results

Key test results are provided in Table 3 and Figure 4. The initial stiffness of SC1 is greater than that for SC2 through SC4, where values were calculated at drift angles less than 0.02%. The

values of the displacements corresponding to the onset of steel faceplate buckling are listed in column 3. Buckling of the faceplates occurred at their free edges prior to achieving the peak load in all four walls. Columns 4 and 5 in the table present computed data for the onset of faceplate yielding, where forces and displacements are calculated using rosette strain gage data and assuming a Von Mises yield criterion. Columns 6 and 7 present peak loads and the corresponding drift angles in the first (positive) and third (negative) quadrants (see Figure 6). Column 8 lists the drift angles at 80% of the peak load in the first and third quadrants.

The initial stiffness of SC3 and SC4 is less than that of the thicker SC1. The initial stiffness of SC2 was substantially less than SC1, which was not expected and is attributed to flexibility at the base of the wall.

Buckling of the faceplates occurred at their free edges prior to achieving peak load, noting that studs were not provided at the vertical free edges of the plates. During subsequent cycles of loading, the plate buckling extended towards the center of wall and was affected by the connector spacing as seen in Figure 7.

Yielding of the faceplates occurs prior to peak load. Peak load is observed at a relatively high drift angle of 1.1+%. The peak loads developed in SC1 and SC2, and SC3 and SC4 are similar, which indicates that connector spacing in the range provided does not impact the peak shearing resistance in flexure-critical walls. The peak loads in SC1 and SC2 are greater than SC3 and SC4 because the infill concrete in SC1 and SC2 is 3 inches thicker. The drift angle at 80% of peak load provides some insight into the importance of the connector spacing (or faceplate slenderness ratio). Given that the walls sustained their peak loads at the same drift angle of 1.18% (7 of 8 per Table 3), the greater the drift angle at 80% peak load, the slower the deterioration of strength with increasing displacement. Wall SC1 has the smallest slenderness ratio of 21 and the greatest drift angle at 80% peak load.

Table 3. Data summary for SC1 through SC4

Specimen	Initial stiffness (kips/in.)	Data point					
		Onset of steel plate buckling	Onset of steel plate yielding		Peak load		Drift angle at 80% peak load (%) Pos/Neg
		Drift angle (%)	Load (kips)	Drift angle (%)	Load (kips)	Drift angle (%) Pos/Neg	
SC1	1680	0.48	240	0.48	317/320	1.18/1.18	2.42/2.56
SC2	1240	0.48	200	0.48	314/319	1.18/1.18	1.85/1.74
SC3	1380	0.70	185	0.48	265/275	1.40/1.18	1.69/1.88
SC4	1310	0.70	200	0.48	270/275	1.18/1.18	1.94/2.40

The cyclic backbone curves of Figure 4 provide further insight into the behavior of these flexure-critical walls. Consider SC1 and SC2, which sustained a similar peak load. The rate of strength deterioration in SC2 post peak load is much greater than in SC1 up to a drift angle of approximately 2.5%, which is attributed directly to faceplate slenderness. Consider SC3 and SC4, which had identical faceplate slenderness: the rate of strength degradation post peak load in the two walls is virtually identical. The load in all four walls at a drift angle of 3.3% was approximately 130 kips. The reason for the more rapid drop in strength of the two thicker walls at the higher drift angles is not yet understood and is being studied at this time.

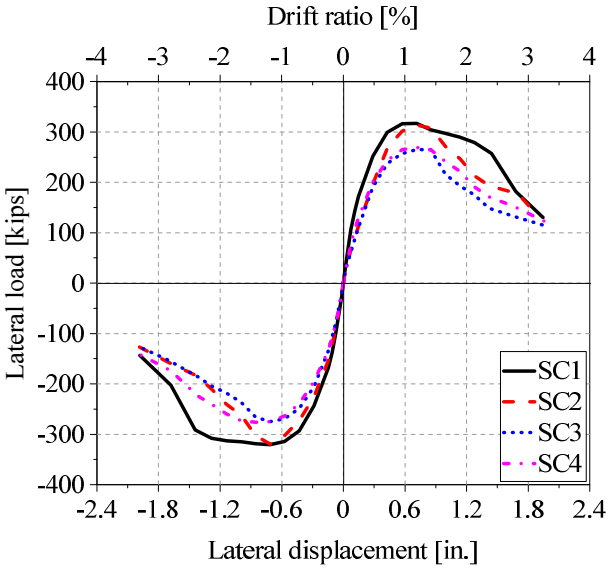

Figure 4. Cyclic backbone curves for the SC walls

Damage to flexure-critical SC walls

Figure 5 provides photographs of damage to SC2. The damage progression in the four SC walls was identical, namely 1) tensile cracking of the concrete at both ends of the wall, 2) outward buckling and yielding of the steel faceplates at the base of the wall, and 3) tearing of the steel faceplates along their welded connection to the base plate. Tearing of the faceplates initiated at drift angles of 1.4% for SC2 and 1.6% for SC1, SC3, and SC4, respectively.

(a) Infill concrete (b) SC wall

Figure 5. Damage to SC2 at 3.3% drift angle

A steel faceplate was removed from each of two specimens, SC2 and SC4, for the purpose of documenting damage to the infill concrete. As seen in Figure 5a, one wide diagonal crack formed in the infill concrete and most of the damage to the infill was concentrated immediately above the base plate, at the level of the first row of tie rods. It is unknown whether the row of connectors immediately above the baseplate represents a potential failure plane, which would have to be addressed in design standards through prescriptive detailing (On-going numerical studies will investigate this issue).

Load-displacement cyclic response

The load-displacement relationships for SC1 through SC4 are shown in Figure 6. The load displacement relationships are similar, with higher peak strengths in the two thicker walls. Pinched hysteresis loops and loss of strength and stiffness are observed for all walls, but occurred at displacements greater than that corresponding to peak strength. The pinching and strength degradation are attributed to faceplate buckling, cracking and crushing of infill concrete, and tearing of the steel faceplate immediately above the baseplate.

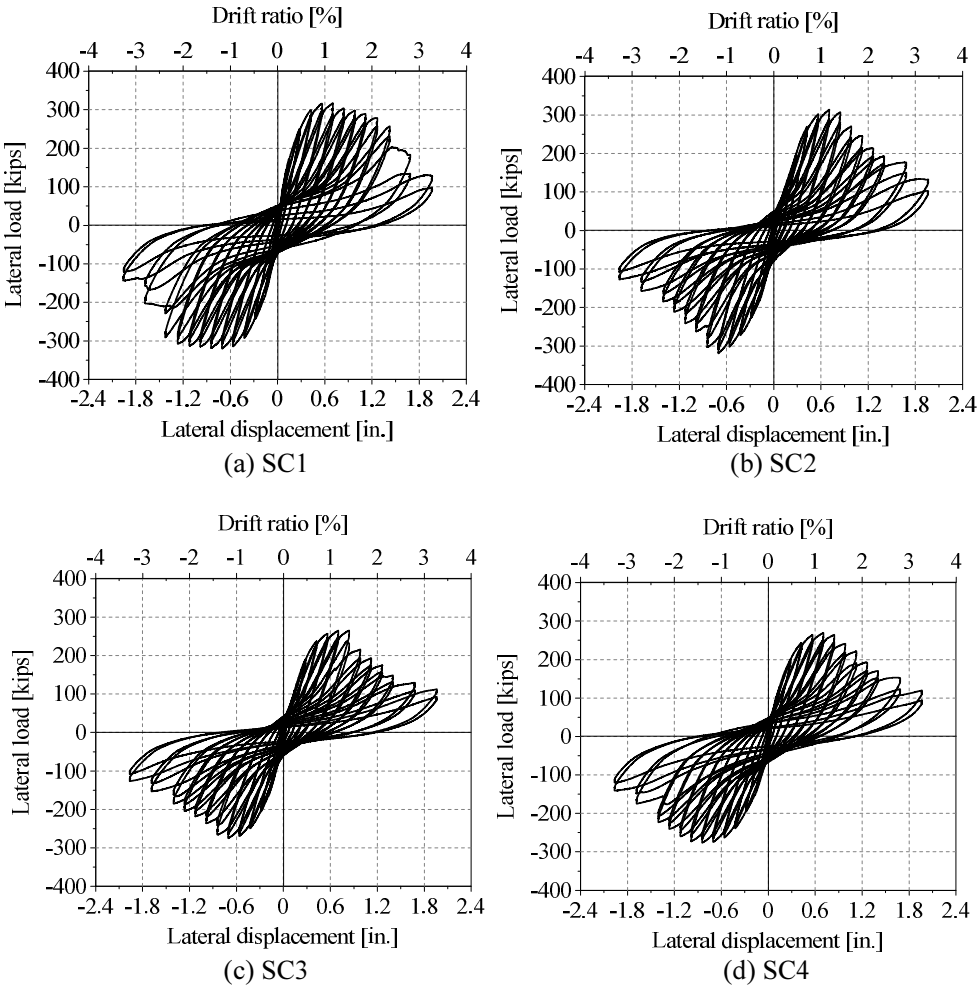

Figure 6. Lateral load - displacement relationships for SC walls

3. NUMERICAL SIMULATION

Finite element models of the test walls were constructed using the general-purpose finite element code ABAQUS (Dassault Systemes, 2012).The material model of multi-axial plasticity theory with Von Mises yield surface, associated flow rules and isotropic hardening was used for steel faceplates. Input parameters for the steel material are the uniaxial stress-strain curve and Poisson's ratio. The concrete damage plasticity model was used to represent the concrete infill, which is based on Drucker-Prager yield surface with non-associated flow. The uniaxial stress-strain curves of concrete in compression and tension together with the parameters of the yield surface are needed to define the material. Four node shell elements were used for the steel faceplates and 3D 8 node solid elements were used for the concrete core and

foundation. The stud bolts and tie rods were modeled using beam elements. Tie constraints were used for the connection of the stud bolts and tie rods to the steel faceplates. The interaction of the stud bolts and tie rods to the concrete infill was represented using the "embedded" option. Half of the ABAQUS model is shown in Figure 7a. Figure 7b enables the comparison of the experiment results to those from the FE model of SC1 under monotonic and cyclic loading.

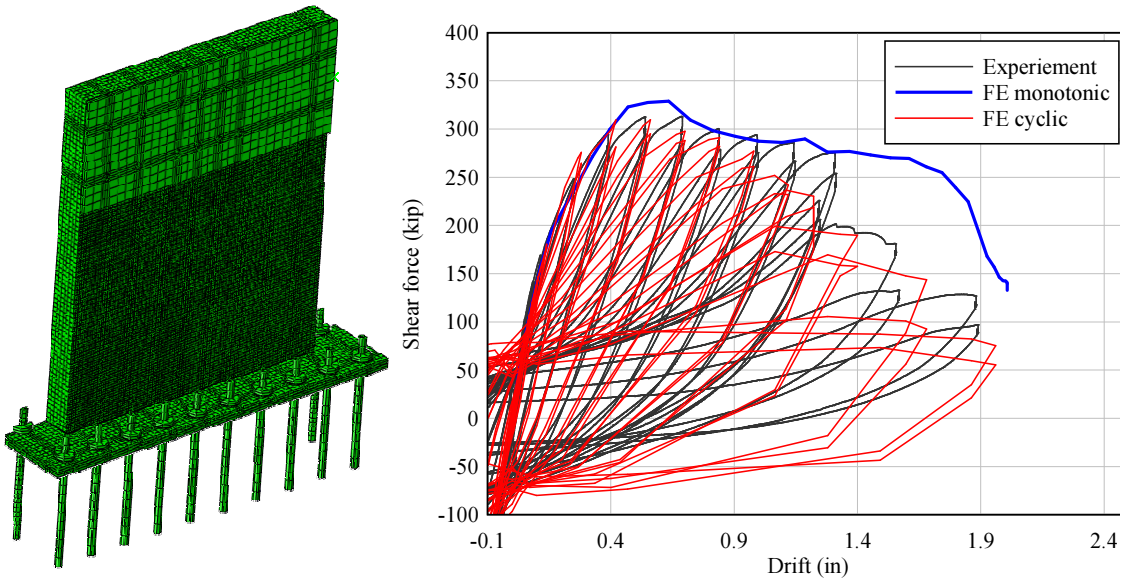

(a) ABAQUS model (b) Numerical and experimental result comparison for SC1

Figure 7. ABAQUS model and results of SC1

The FE model is able to predict reasonably well the experimentally-measured peak strength, the initial stiffness and the hysteresis response of the SC1. The unloading stiffness up to load step 13 is also in good agreement with the experiment results. Computations to walls SC2, SC3 and SC4 are underway.

Initial stiffness

Initial stiffness is an important parameter for the analysis of structural systems incorporating SC walls. The measured and predicted values of initial stiffness for all tested SC walls are presented in Table 3. Column 2 provides the measured initial stiffness of SC walls, where the values were calculated at drift angles of 0.02%. To investigate the effect of foundation flexibility, two sets of ABAQUS models of the SC walls were prepared and analyzed: 1) including all components of the base connection and foundation block, and 2) assuming a rigid connection of the walls to an infinitely stiff base. The ABAQUS predictions of initial stiffness accounting for foundation flexibility recover the measured values very well. The assumption of a rigid base, which would be commonly made by practitioners, would lead to an overestimation of the initial stiffness by a factor of nearly 3.

Table 3. Values of measured and predicted stiffness for SC1 through SC4

Specimen	Measured initial stiffness (kips/in.)	ABAQUS predictions	
		Rigid base (kips/in.)	Flexible base (kips/in.)
SC1	1680	4310	1550
SC2	1240	4300	1500
SC3	1380	4170	1260
SC4	1310	4100	1390

4. CLOSING REMARKS

Four large-scale SC walls (SC1 through SC4) were constructed at the NEES facility at the University at Buffalo as part of a NSF-funded NEES project on low aspect ratio conventional and composite shear walls. The walls had an aspect ratio of 1.0 and were flexure critical. The walls were tested under reversed cyclic loading. The design space for the walls included reinforcement ratio and faceplate slenderness ratio. A bolted baseplate to RC foundation connection was used for all four walls.

The key findings of this study to date are:

1. The four flexure-critical walls sustained peak loads close to that predicted by pre-test calculations using commercially available software. Faceplate slenderness ratio did not influence the peak resistance of the walls, for the range of ratio studied (21 to 32).
2. The damage progression in the four walls was identical, namely cracking and crushing of infill concrete at the toes of the walls, outward buckling and yielding of the steel faceplates near the base of the wall, and tearing of the faceplates at their junction with the base plate. Buckling of the faceplates would have been delayed if a vertical row of studs had been provided near the boundaries of the walls.
3. Pinched hysteresis and loss of stiffness and strength was observed in all four walls at lateral displacements greater than that corresponding to peak load.
4. The damage to the infill concrete was concentrated in the region immediately above the baseplate and at and below the first row of connectors in all four walls.
5. The post-peak response of flexure-critical SC walls is influenced by faceplate slenderness ratio, with a smaller rate of degradation post peak load observed in the wall with the smallest faceplate slenderness ratio.
6. Numerical studies of initial stiffness showed the importance of addressing foundation flexibility. Including foundation flexibility enabled the ABAQUS calculations of initial stiffness to match the measured values well. Ignoring the foundation flexibility would lead to an overestimation of the initial stiffness by a factor of 3, which would have a significant impact on the computations of demand on structural components and safety-related secondary systems.
7. Numerical results using ABAQUS were in good agreement with the experiment data. Further validation with other test data is needed to provide confidence in using FE models in design and assessment of SC walls.

ACKNOWLEDGEMENTS

This project was supported in part by the US National Science Foundation under Grant No. CMMI-0829978. This support is gratefully acknowledged. We also thank NEES laboratory

technical staff at the University of Buffalo, the technical staff at the Bowen Laboratory, and the staff of LPCiminelli Inc. for their contributions to the project.

REFERENCES

AISC N690 (2006). Specification for safety-related steel structures for nuclear facilities. AISC, Chicago, IL.

Dassault Systemes (2012). ABAQUS v6.12. Providence, RI, USA.

Fukumoto, T., Kato, B., Sato, K., Toyama, K., Kobayashi, M., Emori, K., Ishii, K. and Sakamoto, M. (1987). "Concrete filled steel bearing walls." IABSE 5.

JEAG-4618 (2005). Technical guidelines for aseismic design of steel plate reinforced concrete structures. Japan Electric Association.

Kaneuji, A., Okuda, Y., Hara, K. and Hasumoto, H. (1989). Feasibility study of concrete filled steel (SC) structure for reactor buildings. Transactions of the 10th SMiRT. H**:** 67-72.

Ozaki, M., Akita, S., Osuga, H., Nakayama, T. and Adachi, N. (2004). "Study on steel plate reinforced concrete panels subjected to cyclic in-plane shear." Nuclear Engineering and Design 228(1-3): 225-244.

Sasaki, N., Akiyama, H., Narikawa, M., Hara, K., Takeuchi, M. and Usami, S. (1995). Study on a concrete filled steel structures for nuclear power plants (part 3). Shear and bending loading tests on wall members.

Takeda, T., Yamaguchi, T., Nakayama, T., Akiyama, H. and Katao, Y. (1995). Experimental study on shear characteristics of a concrete filled steel plate wall, Brazil.

Varma, A. H., Zhang, K., Chi, H., Booth, P. and Baker, T. (2011). In-plane shear behavior of SC composite walls: Theory vs. Experiment. Transactions, SMiRT 21. New Delhi, India**:** Div-VI: Paper ID# 764.

APPENDIX

Table A-1. Unit conversion table

Quantity	U.S. Unit	SI equivalent
Length	1 in	0.0254 m
	1 ft	0.3048 m
Force	1 lbf	4.4482 N
	1 kip	4.4482 kN
Stress	1 psi	6894.8 Pa (N/m^2)
	1 ksi	6894.8 kPa (kN/m^2)